

# Speed Planning for Solar-Powered Electric Vehicles

Mingsong Lv

Northeastern University, China  
lumingsong@cse.neu.edu.cn

Nan Guan

The Hong Kong Polytechnic  
University  
csguannan@comp.polyu.edu.hk

Ye Ma

Northeastern University, China  
mayeneu@gmail.com

Dong Ji

BMW Brilliance Automotive Ltd.  
dong.ji@bmw-brilliance.cn

Erwin Knippel

BMW Brilliance Automotive Ltd.  
erwin.knippel@bmw-brilliance.cn

Xue Liu

McGill University, Canada  
xueliu@cs.mcgill.ca

Wang Yi

Uppsala University, Sweden  
yi@it.uu.se

## ABSTRACT

Electric vehicles (EVs) are the trend for future transportation. The major obstacle is range anxiety due to poor availability of charging stations and long charging time. Solar-powered EVs, which mostly rely on solar energy, are free of charging limitations. However, the range anxiety problem is more severe due to the availability of sun light. For example, shadings of buildings or trees may cause a solar-powered EV to stop halfway in a trip. In this paper, we show that by optimally planning the speed on different road segments and thus balancing energy harvesting and consumption, we can enable a solar-powered EV to successfully reach the destination using the shortest travel time. The speed planning problem is essentially a constrained non-linear programming problem, which is generally difficult to solve. We have identified an optimality property that allows us to compute an optimal speed assignment for a partition of the path; then, a dynamic programming method is developed to efficiently compute the optimal speed assignment for the whole trip with significantly low computation overhead compared to the state-of-the-art non-linear programming solver. To evaluate the usability of the proposed method, we have also developed a solar-powered EV prototype. Experiments show that the predictions by the proposed technique match well with the data collected from the physical EV. Issues on practical implementation are also discussed.

## Keywords

speed planning; electric vehicle; solar

## 1. INTRODUCTION

*Electric vehicles* (EVs) are considered one of the future means of transportation since they use electricity which can

be obtained from many renewable energy sources, such as tidal power, solar power, and wind power. Besides, EV has the flexibility to integrate many different energy generators, such as solar panels and fuel cells [27]. Regarding the US market, the PEV and EV sales doubles every year from 2011 to 2013 [11]. A 20% steady increase of annual growth rate of the global EV market is predicted before 2020 [7].

Wide acceptance of EVs still faces several challenges. For now, the limited range of common EVs is considered to be a major obstacle. Small battery capacity together with a sparse availability of charging stations and hour-scale charging time makes long-range journey infeasible, which is widely termed *range anxiety* to express the driver's fear of fully depleting the batteries during a trip [24].

A special class of EV is *solar-powered EV*, which partly or totally relies on solar energy (obtained from the solar panels installed on the car) to propel the vehicle. Solar-powered EVs are considered a solution for sustainable mobility within duty ranges [29, 30], since they may collect energy when not only parking but also travelling on the road. Although charging limitation is not as urgent, the range anxiety problem is even more severe due to unpredictable solar input. For example, when driving on urban roads, one may encounter intermittent shadings by buildings or trees, in which very little solar energy can be harvested.

Recently, speed and route planning [8] was proposed as a solution to the range anxiety problem for ordinary EVs. The main idea is to choose a path and assign proper speeds so that the energy consumption is minimized for a given trip. However, speed planning for solar-powered EVs is much more complex due to the availability of sunshine. The driver has to survive the shaded road segments of a trip where there is little solar input. Furthermore, energy consumption is very often coupled with timing requirements, such as deadlines. Users in most cases have to face the trade-off between travel time and energy consumption.

In this paper, we study the problem of speed planning for solar-powered EVs so that one can complete a given trip with minimal travel time. This is essentially a complex constrained non-linear programming problem with multiple variables which, in general, cannot be efficiently solved. We identified an optimality structure of the specific problem, which enables us to compute the optimal speeds for partitions of the whole path without losing global optimality.

Permission to make digital or hard copies of all or part of this work for personal or classroom use is granted without fee provided that copies are not made or distributed for profit or commercial advantage and that copies bear this notice and the full citation on the first page. Copyrights for components of this work owned by others than ACM must be honored. Abstracting with credit is permitted. To copy otherwise, or republish, to post on servers or to redistribute to lists, requires prior specific permission and/or a fee. Request permissions from [permissions@acm.org](http://permissions.acm.org).

*e-Energy '16 June 21–24, 2016, Waterloo, Canada*

© 2016 ACM. ISBN 123-4567-24-567/08/06...\$15.00

DOI: <http://dx.doi.org/10.1145/2934328.2934334>

Then a dynamic programming method is used to find the actual partition. Simulation results show that in terms of analysis efficiency, our approach significantly outperforms a standard non-linear programming solver that applies global searching of the optimal speed assignment.

We also developed a solar-powered EV prototype to validate the quality of the proposed method in complicated real-life scenarios. Experimental results show that the predictions by our approach, such as the amount of harvested energy, are generally close to those obtained from the physical solar-powered EV.

We acknowledge that the proposed solar solution is not (and never will be) applicable to ordinary EVs, which weigh around 2 tons, mainly because the planned speed is too slow. However, the solution could be useful in the future on low-speed EVs (or neighbourhood EVs) with improved efficiency of solar panels.

## 2. SYSTEM MODELS

In this section, we present the trip path model, the energy input and output models of a solar-powered EV.

### 2.1 Path Model

A path from starting point to destination is composed of alternative *illuminated road segments* and *shaded road segments* according to the availability of sunshine. Note that shadings can be caused by vast factors, such as tall buildings, trees along the road, hills, tunnels, etc. Without loss of generality, a path can be defined as follows:

DEFINITION 1 (PATH; MACRO SEGMENT; SEGMENT). *A path from location A to location B is composed of n consecutive macro (road) segments,*

$$\mathcal{P}(A, B) = \langle S_1, S_2, \dots, S_n \rangle \quad (1)$$

where each macro segment  $S_i$  is further composed of an illuminated segment  $S_i^I$  followed by a shaded segment  $S_i^S$ .

$$S_i = \langle S_i^I, S_i^S \rangle \quad (2)$$

Thus, a path can also be written as:

$$\mathcal{P}(A, B) = \langle S_1^I, S_1^S, S_2^I, S_2^S, \dots, S_n^I, S_n^S \rangle \quad (3)$$

A path may start with a shaded road segment in practice. This can be treated as a macro road segment with an infinitely small leading illuminated segment. In this case, the EV must rely on an initial energy buffer to survive the first shaded segment. We do not further divide a single (illuminated or shaded) segment into smaller segments.

### 2.2 Solar Energy Input Models

In this paper, we consider EVs equipped with both solar panels and batteries. The solar panels serve as the main energy input, and the batteries are used as a buffer to temporarily store unused solar energy, collected either before or during the trip. At the beginning of a trip, the total available energy in the batteries is represented by  $E_0$ . On illuminated road segments, solar energy is the main energy source. The batteries may be used as an auxiliary source or to store excess energy according to the amount of solar input. On shaded road segments, energy consumption solely depends on the batteries.

We assume perfect batteries by which the available amount of energy does not decrease when the batteries are discharging with high current (i.e., high power output). Thus, the available energy at any time can be totally used to drive the EV regardless of its instantaneous power requirement.

Solar power changes over time with the sun angle during the daytime [23]. The actual power output of a solar panel is a fraction of the total solar power, which is determined by the cell efficiency of the panel. Nowadays, the average cell efficiency of commercial solar panel products (based on single crystal or multicrystalline) is around 20%, and that of multi-junction photovoltaic cells can reach up to 46% [5]. Since solar irradiance is continuously changing, Maximal Power Point Tracking (MPPT) controllers are installed to optimize solar power output.

In this paper, we assume constant solar power input for illuminated segments,  $\mathbf{c}$  in equation 4. The assumption is reasonable for short trips, e.g., an hourly trip from home to office. We apply the lowest solar power within the deadline of a trip to ensure safe predictions. For shaded road segments,  $\mathbf{c} = 0$ . The total energy input for an illuminated segment of length  $S$  with constant cruising speed  $\mathbf{V}$  is:

$$\mathbf{E}in = \mathbf{c} \cdot \frac{S}{\mathbf{V}} \quad (4)$$

### 2.3 EV Energy Consumption Models

We intend to establish the relationship between the cruising speed and the energy consumption of an EV on a give road segment. Energy consumption is in principle an integration of the power output ( $\mathbf{P}out$ ) within a time interval. Given a trip starting at time  $t_0$  and ending at  $t_1$ , the energy consumption is expressed by equation (5).

$$\mathbf{E}out = \int_{t_0}^{t_1} \mathbf{P}out dt \quad (5)$$

For propelling, the instantaneous power output is mainly used to overcome (i) rolling and hill climbing resistance, (ii) aerodynamic drag, and to provide (iii) acceleration, which are expressed as the main components of equation (6) [15]. In practice, power loss exists in both mechanical and electrical sub-systems, so their efficiencies,  $\eta_m$  and  $\eta_e$  respectively ( $0 < \eta_m, \eta_e < 1$ ), are also included. Detailed meanings of the physical parameters can be found in [15]. Clearly, cruising speed ( $\mathbf{V}$ ) plays a key role in determining the power output of an EV.

$$\mathbf{P}out = \frac{\mathbf{V}}{\eta_m \eta_e} (M(f_r + i) + \frac{1}{2} \rho_a C_D A_f \mathbf{V}^2 + M \delta \frac{d\mathbf{V}}{dt}) \quad (6)$$

In this paper, we consider such a model in which acceleration power is not incurred (In Sec. 5, experimental results show this assumption is reasonable in real-life settings). Thus, the transient power output at speed  $\mathbf{V}$  is expressed by equation 7, where parameters  $a$  and  $b$  are determined by the vehicle itself and the road conditions. If the EV runs at a constant speed  $\mathbf{V}$  within distance  $S$ , the energy consumption is expressed by equation 8.

$$\mathbf{P}out = a\mathbf{V}^3 + b\mathbf{V} \quad (7)$$

$$\mathbf{E}out = S(a\mathbf{V}^2 + b) \quad (8)$$

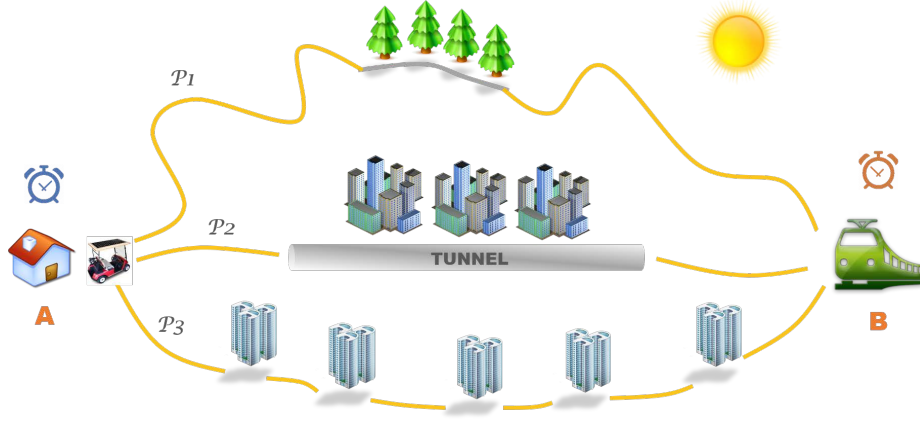


Figure 1: A motivating example for speed planning

### 3. THE SPEED PLANNING PROBLEM

To explain the speed planning problem, consider the scenario depicted in Figure 1. A person starts from home ( $A$ ) for the railway station ( $B$ ) at a specific time  $t$  on daytime, driving a solar-powered EV. There are three path options,  $\mathcal{P}_1$ ,  $\mathcal{P}_2$  and  $\mathcal{P}_3$ , by choosing which the driver is concerned about (i) whether he can successfully arrive at the destination, and moreover (ii) whether the trip can be finished in time so that he does not miss the train.

Given no traffic jams, and for a traditional combustion engine vehicle or a battery-powered EV, the driver may probably choose the shortest path  $\mathcal{P}_2$  to save time. However,  $\mathcal{P}_2$  includes a long tunnel to avoid a densely populated area. Now, for a solar-powered EV, it will get no energy input underground, which means the vehicle could probably stop half-way in the tunnel. Comparably, other longer paths, such as  $\mathcal{P}_1$  with a small shaded segment and ample solar input for the overall path, seem to be feasible.

More importantly, one must carefully plan his speed on the path. Take  $\mathcal{P}_2$  for example, to successfully survive the “dark” tunnel, the driver has to collect enough energy by driving very slowly on the illuminated segment before entering the tunnel. In the tunnel, the driver may decide to drive very fast to leave the “dangerous” segment as soon as possible. However, this can be a bad decision: driving too fast will very quickly deplete the precious collected energy, because the faster the EV runs, the more energy it will consume (as shown by equation (8)).

Furthermore, the driver is faced with a harder problem: to balance the speeds between the illuminated segment and the shaded segment. He can drive faster on the illuminated segment to save time, which nevertheless reduces the amount of collected energy, limiting his speed in the shaded segment. The situation is even more complex if many illuminated and shaded segments interleave with each other, like on path  $\mathcal{P}_3$ .

As can be seen, intuitions and experience in planning trip for traditional combustion engine vehicles and battery-powered EVs do not apply for solar-powered EVs. The driving speed must be systematically planned according to complex road situations and vehicle conditions, so that the driver can successfully complete the trip and meet timing requirements.

To assign a speed to each road segment to achieve minimal overall travel time is a very complex constrained optimiza-

tion problem, which can be formally expressed as follows:

**THE SPEED PLANNING PROBLEM**

**Objective function:**

$$T_{min} = \min \sum_{i=1}^n (\mathcal{T}(S_i^I, \Omega(S_i^I)) + \mathcal{T}(S_i^S, \Omega(S_i^S)))$$

**Constraints:**

$\forall i \in \{1..n\}, * = \{I, S\} \quad \Omega(S_i^*) > 0;$

$\forall i \in \{1..n\}, * = \{I, S\} \quad E_i^* \geq 0;$

(i) for an illuminated segment,  
 $E_i^I = E_{i-1}^S + \mathbf{E}in_i^I - \mathbf{E}out_i^I \geq 0;$

(ii) for a shaded segment,  
 $E_i^S = E_i^I - \mathbf{E}out_i^S \geq 0$

The travel time of a path can be expressed by the sum of the times spent in each illuminated or shaded segment. In the objective function,  $\Omega(S_i^*)$  is a positive speed assignment function for a given road segment  $S_i^*$ , and  $\mathcal{T}(S_i^*, \Omega(S_i^*))$  is the function to compute the travel time given  $\Omega(S_i^*)$ . To find the optimal speed profile, i.e.,  $\Omega(S_i^*)$  for each road segment, the major difficulty is that the speed of a segment may depend on other segments, as explained previously.

If the EV can successfully arrive at the destination, the remained energy at the end of each road segment,  $E_i^*$ , must be non-negative, as expressed by the constraints.  $\mathbf{E}in$  and  $\mathbf{E}out$  are computed by equations (4) and (8) respectively. Note that inequality (ii) actually dominates inequality (i): if (ii) is true, then (i) must hold since  $\mathbf{E}out_i^S \geq 0$ . Then it suffices to only constrain the remained energy at the end of each *macro segment*.

The best path can be determined by comparing the minimal travel times for all available paths from location  $A$  to location  $B$ , the number of which is typically not big in practice. So in this paper, we focus our discussion on optimizing the travel time for a single path.

### 4. OPTIMAL SPEED PLANNING

To obtain the optimal solution efficiently, we decompose the problem into several sub-problems to tackle the difficulty step-by-step:

(1) *Optimal speed assignment for a single macro segment:* We find that the optimal speed assignment for a macro

segment is to maintain a constant speed within each (illuminated or shaded) segment. Computing the speeds can be formulated into a small-scale constrained non-linear programming problem which can be efficiently solved.

(2) *Optimal speed assignment for multiple macro segments:* When assigning speed for multiple macro segments, the complexity increases significantly. For our problem, we find that when the global optimal solution is achieved, the speed assignment actually exhibits an interesting property: the whole path is partitioned into several chunks with each chunk containing several macro segments: the remained energy at the end of each chunk is zero, and within a chunk, the macro segments have the same speed assignment. By this, we can treat all the macro segments in a chunk as a single big macro segment, and thus speed assignment can be reduced to solving the big segment.

(3) *Optimal speed assignment for the whole path by dynamic programming:* Now, computing the optimal speed assignment for a whole path can be decomposed into computing several chunks. However, we still do not know where these zero-energy points actually locate in the path. A naïve way is to enumerate all possibilities, but the complexity is exponential. By the optimal structure of our problem, we present a dynamic programming based method to systematically find these points with polynomial complexity.

## 4.1 Speed Planning for a Macro Segment

First, consider the speed assignment for a single illuminated/shaded segment, we have the following lemma.

LEMMA 1. *Given a specific energy consumption  $E$ , the minimal travel time for a road segment with length  $S$  is achieved by maintaining a constant speed.*

PROOF. An EV may move at variable speeds on a road segment. This behavior can be modeled as: the road segment  $S$  is partitioned into  $n$  consecutive parts ( $S_1$  to  $S_n$ ), in each of which the EV moves at a constant speed  $x_i$ . The modeling is precise since we do not pose limitations on either the length of each  $S_i$  or the number of partitions. Now the total energy consumption on  $S$  is  $E = \sum_{i=1}^n S_i(ax_i^2 + b)$ .

Let  $f(x_1, \dots, x_n) = T = \sum_{i=1}^n \frac{S_i}{x_i}$ , and

$g(x_1, \dots, x_n) = \sum_{i=1}^n S_i(ax_i^2 + b) - E$ .

To minimize  $f(x_1, \dots, x_n)$  subject to  $g(x_1, \dots, x_n) = 0$ , we apply the method of *Lagrange multipliers* [10], which introduces a constant  $\lambda$  ( $\lambda \geq 0$ ) and an auxiliary function:

$\Lambda(x_1, \dots, x_n, \lambda) = f(x_1, \dots, x_n) + \lambda g(x_1, \dots, x_n)$ .

The values of the variables leading to the minimum of  $f$  can be obtained by computing the equation set:

$\nabla_{x_1, \dots, x_n, \lambda} \Lambda(x_1, \dots, x_n, \lambda) = 0$ , where  $\nabla_{x_i} \Lambda = \frac{\partial \Lambda}{\partial x_i}$ .

By the symmetry of the representations of  $f$  and  $g$ , for any  $i$ ,  $\nabla_{x_i} \Lambda(x_1, \dots, x_n, \lambda)$  are the same, and at the optimal point,  $x_i = \sqrt[3]{\frac{1}{2a\lambda}}$ ,  $i = 1 \dots n$ . This means the trip time  $T$  reaches its minimum when the speeds for all  $S_i$  are the same, i.e., a constant speed for the whole road segment.  $\square$

Then consider the optimal speed assignment for a macro segment, we have the following result.

THEOREM 1. *Given a macro segment  $S$  with an illuminated segment of length  $S_1$  and a shaded segment of length*

*$S_2$ , the energy at the beginning and the end of  $S$  is  $E_0$  and  $E_1$  respectively. The minimal travel time is achieved when  $S_1$  and  $S_2$  are assigned constant speed respectively.*

PROOF. Since a solar-powered EV in a shaded segment relies on the energy transferred from its previous illuminated segment, we assume that at the end of  $S_1$ ,  $E_2$  amount of energy is transferred to  $S_2$ . The energy consumed in  $S_1$  is  $E_0 + \mathbf{E}in - E_2$ , where  $\mathbf{E}in$  is the harvested energy in  $S_1$ , which is determined by the travel time  $t$  in  $S_1$ . Energy consumption in  $S_2$  is  $E_2 - E_1$ . By Lemma 1, the most time saving approach is to run at a constant speed in both  $S_1$  for any valid  $t$ , and also run at a constant speed in  $S_2$ .  $\square$

Lemma 1 and Theorem 1 exhibit the properties when minimal travel time is achieved for a macro segment. To find the actually speed values in  $S_1$  and  $S_2$ , one can use constrained non-linear programming solvers in practice.

## 4.2 Key Properties for the Optimal Speed Assignment

Now we consider to find the optimal speed assignment for a path. We use  $x_i^*$  to represent the speed assigned to each segment  $S_i^*$ , and use  $\bar{x}_i^*$  to represent the point at which the objective function reaches its global minimum. The objective function to be optimized and the set of inequality constraints are expressed as follows:

$$f(x_1^I, x_1^S, \dots, x_n^I, x_n^S) = \sum_{i=1}^n \left( \frac{S_i^I}{x_i^I} + \frac{S_i^S}{x_i^S} \right) \quad (9)$$

$$\forall k = 1..n, \quad g_k(x_1^I, x_1^S, \dots, x_n^I, x_n^S) = \sum_{i=1}^k \{ [S_i^I(a(x_i^I)^2 + b)] + [S_i^S(a(x_i^S)^2 + b)] \} - \sum_{i=1}^k c \frac{S_i^I}{x_i^I} - E_0 \leq 0 \quad (10)$$

The above problem is much more complex than optimization for a single macro segment, mainly due to the interdependency between different macro segments. For example, consider two consecutive macro segments  $S_1$  and  $S_2$ :  $S_1$  contains a long illuminated segment and a short shaded segment; the configuration of  $S_2$  is the opposite. Then  $S_1$  may transfer energy to feed the long shaded segment in  $S_2$ .

The complex optimization problem can be directly solved by existing non-linear programming solvers. However, the performance of such a method does not scale with the number of macro segments.

In our research, we find that when an optimal speed assignment for a path is reached, the remained energy at the end of some macro segments is 0. For two adjacent zero-energy points, all the macro segments included have the same speed profile. This property is formulated into Theorem 2 and proved as follows.

THEOREM 2. *For any  $i$  and  $j$ , if the remained energy at the end of macro segments  $i - 1$  and  $j$ , is 0, denoted by  $E_{i-1} = E_j = 0$ , and for any  $k$  ( $i \leq k < j$ )  $E_k > 0$ , then  $x_i^I = x_{i+1}^I = \dots = x_j^I$  and  $x_i^S = x_{i+1}^S = \dots = x_j^S$ , when the minimal travel time for the path is reached.*

PROOF. By Karush-Kuhn-Tucker necessary conditions [10] for a non-linear optimization problem, when the function  $f$

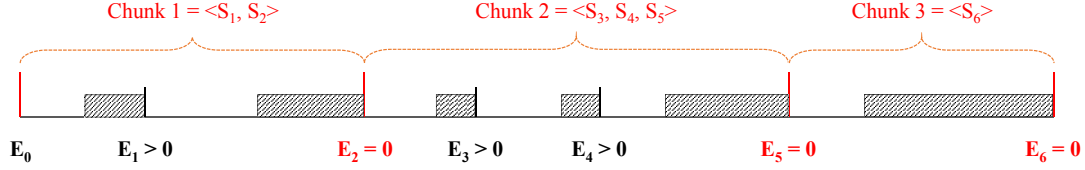


Figure 2: An example of chunks separated by zero-energy points

(equation (9)) subject to a set of  $n$  constraints  $g_i \leq 0$  ( $i = 1, \dots, n$ ) (expressed by (10)) reaches its minimum, and  $f$  and  $g$  satisfy some regularity conditions<sup>1</sup>, then there exist constants  $\mu_i$  ( $i = 1, \dots, n$ ), such that:

$$\nabla f(\bar{X}) + \sum_{i=1}^n \mu_i \nabla g_i(\bar{X}) = 0 \quad (11)$$

$$\mu_i g_i(\bar{X}) = 0 \quad \text{for } i = 1, \dots, n \quad (12)$$

$$\mu_i \geq 0 \quad \text{for } i = 1, \dots, n \quad (13)$$

Here we use  $\bar{X}$  to symbolically represent the set of variables  $\{\bar{x}_i^* | i = 1, \dots, n, * = I \text{ or } S\}$ , i.e., the optimal speed assignment for simplicity.

Expending equation set (11), we obtain two sets of equations, for  $i = 1, \dots, n$ :

$$-\frac{S_i^I}{(\bar{x}_i^I)^2} + \left( \sum_{k=i}^n \mu_k \right) \cdot (2a S_i^I \bar{x}_i^I + \frac{c S_i^I}{(\bar{x}_i^I)^2}) = 0 \quad (14)$$

$$-\frac{S_i^S}{(\bar{x}_i^S)^2} + \left( \sum_{k=i}^n \mu_k \right) \cdot (2a S_i^S \bar{x}_i^S) = 0 \quad (15)$$

By solving the above sets of equations we get

$$(\bar{x}_i^I)^3 = \frac{1}{2a \sum_{k=i}^n \mu_k} - \frac{c}{2a} \quad (16)$$

$$(\bar{x}_i^S)^3 = \frac{1}{2a \sum_{k=i}^n \mu_k} \quad (17)$$

So for any macro segment  $S_i$ , if the remained energy at the end of it is not zero, which is equivalent to  $g_i(\bar{X}) < 0$ , then “ $\mu_i = 0$ ” must hold, from equations (12) and (13).

Now considering macro segment  $S_i$  and  $S_{i+1}$ , if  $g_i(\bar{X}) < 0$ , from equations (16) and (17), we can see that:

$$\bar{x}_i^I = \bar{x}_{i+1}^I, \text{ and } \bar{x}_i^S = \bar{x}_{i+1}^S.$$

Then, all the macro segments between two adjacent zero-energy points have the same speed assignment<sup>2</sup>.  $\square$

<sup>1</sup>Let  $\bar{x}$  be a feasible solution, and denote  $I = \{i : g_i(\bar{x}) = 0\}$ , if (i)  $f$  and  $g_i$  are differentiable at  $\bar{x}$ , (ii)  $g_i$  for  $i \notin I$  are continuous at  $\bar{x}$ , and (iii)  $\nabla g_i(\bar{x})$  for  $i \in I$  are linearly independent, then conditions (12)-(14) apply. Proof provided in: [faculty.neu.edu.cn/ise/lvmingsong/e-energy2016/kkt-proof.pdf](http://faculty.neu.edu.cn/ise/lvmingsong/e-energy2016/kkt-proof.pdf)

<sup>2</sup>For macro segment  $S_i$  with  $g_i(\bar{X}) = 0$ , i.e., the remained energy at its end is zero, one cannot determine whether  $\mu_i = 0$ . If  $\mu_i = 0$ , the above results for  $S_i$  and  $S_{i+1}$  also hold.

Note that the remained energy at the end of the path must be zero. The result is trivial: if there is remained energy in the end, we can at least use it in the last shaded segment to further reduce the overall travel time. So the optimal solution always implies that the energy at the end of the path is depleted.

With Theorem 2, we know that when the optimal point is reached, there must be some macro segment end point(s) with zero remained energy, and these points divide the whole path into several big chunks, as shown in Figure 2. This motivates us with a simpler way to compute the optimal solution. If by some methods the zero-energy points within a path can be exactly located, we can construct a new macro segment  $\hat{S} = \langle \hat{S}^I, \hat{S}^S \rangle$ , where  $\hat{S}^I = \sum S_i^I$  and  $\hat{S}^S = \sum S_i^S$ , for any  $S_i$  in the same chunk. A non-linear programming solver can be used to compute the optimal speed assignment for  $\hat{S}$ . Note that computing the optimal speed assignment for one single macro segment is much cheaper than for a series of consecutive macro segments. Now the remained problem is how to find the zero-energy points.

### 4.3 Finding Optimal Speed Profile by Dynamic Programming

A major difficulty in finding the chunk separation points is that we do not even know how many such points actually exist in a path. A naïve method would be to enumerate all possible combinations in the path. However, the complexity of such a method is exponential. In this section, we present a dynamic-programming-based method to search the separation points in polynomial time.

Given a path  $\mathcal{P} = \langle S_1, \dots, S_N \rangle$  with  $N$  macro segments, we introduce  $N - 1$  variables  $c_1, \dots, c_{N-1}$ , with  $1 \leq c_i \leq c_{i+1} \leq N$  for any  $i = 1 \dots N - 2$ , as the *separation points* of  $\mathcal{P}$ . An assignment of values to  $c_1, \dots, c_{n-1}$  refers to a *partition* of  $\mathcal{P}$  into  $N$  chunks. Specially, we define  $c_0 = 0$  and  $c_N = N$  to represent the start and end points of path  $\mathcal{P}$ . When there are less than  $N$  chunks regarding an optimal solution, some separation points must have the same value. We use  $t_{cs}(c_i, c_j)$  to denote the optimal travel time for a chunk between  $c_i$  and  $c_j$ .

We then define a function  $\mathbf{Opt}(x)$  which gives a way to compute the travel time for a sub-path starting from the  $x$ -th macro segment and ending with the end of the path. For such a sub-path, we need  $N - x$  separation points  $c_x, c_{x+1}, \dots, c_{N-1}$ . We use  $c_{x-1}$  and  $c_N$  to refer to the starting point and the end point of the sub-path.

$$\mathbf{Opt}(x) = \min_{\substack{\forall x \leq c_x \leq N \\ \forall c_x \leq c_{x+1} \leq N \\ \dots \\ \forall c_{N-2} \leq c_{N-1} \leq N}} \left\{ \sum_{k=x}^N t_{cs}(c_{k-1}, c_k) \right\} \quad (18)$$

**THEOREM 3** (OPTIMALITY OF  $\mathbf{Opt}(x)$ ).  $\mathbf{Opt}(x)$  returns the global minimal travel time for path  $\mathcal{P} = \langle S_x, \dots, S_N \rangle$ .

**PROOF.** By the definition of  $\mathbf{Opt}(x)$ , it is easy to see that it covers all possible number of actual separation points and for each number all possible assignments.  $\square$

From the definition of  $\mathbf{Opt}$  and Theorem 3, we have

$$\begin{aligned} \mathbf{Opt}(1) &= \min_{\substack{\forall 1 \leq c_1 \leq N \\ \forall c_1 \leq c_2 \leq N \\ \dots \\ \forall c_{N-2} \leq c_{N-1} \leq N}} \left\{ \sum_{k=1}^N t_{cs}(c_{k-1}, c_k) \right\} \\ &= \min_{\forall 1 \leq c_1 \leq N} \{ t_{cs}(0, c_1) + \mathbf{Opt}(c_1 + 1) \} \end{aligned} \quad (19)$$

Note that  $\mathbf{Opt}(N + 1) = 0$ . The above equation implies that the original optimization problem can be recursively reduced to a simpler problem which is easier to solve. So we present a dynamic-programming-based algorithm as follows.

---

**Algorithm 1** Optimal Speed Planning for a Path

---

**Input:** (1) the path  $\mathcal{P}(A, B) = \langle S_1, S_2, \dots, S_N \rangle$ ; (2) initial energy in the buffer:  $E_0$

**Output:** Optimal speed assignment to each road segment

```

1: /* STEP 1: compute the optimal travel times for all
   possible chunks */
2: for  $i = 1 \rightarrow n$  do
3:   for  $j = i \rightarrow n$  do
4:     compute  $t_{cs}(i, j)$  for chunk  $[i, j]$ 
5:     if chunk  $[i, j]$  is NOT valid then
6:        $t_{cs}(i, j) = +\infty$ 
7:     end if
8:   end for
9: end for
10: /* STEP 2: compute  $\mathbf{Opt}(i)$  bottom up */
11:  $\mathbf{Opt}(N) = t_{cs}(N, N)$ 
12: for  $i = N - 1 \rightarrow 1$  do
13:    $\mathbf{Opt}(i) = +\infty$ 
14:   for  $j = i \rightarrow N$  do
15:      $\mathbf{Opt}(i) = \min\{\mathbf{Opt}(i), t_{cs}(i, j) + \mathbf{Opt}(j + 1)\}$ 
16:   end for
17:   Record the speed assignment of  $\mathbf{Opt}(i)$ 
18: end for
19: return  $\mathbf{Opt}(1)$ 

```

---

Algorithm 1 contains two main steps. First, we pre-compute the travel times for all possible chunks, which are used to compute  $\mathbf{Opt}(i)$ , ( $i = N \dots 1$ ) in the second step. Note that line 5 involves a process to validate a chunk  $[i, j]$ , in which we compute the remained energy for each macro segment within chunk  $[i, j]$ , given the computed speed assignment and the initial energy ( $E_0$  if  $i = 1$ ; 0 otherwise). If there is at least one macro segment whose remained energy is negative, then chunk  $[i, j]$  represents an invalid partition in the problem domain. It is easy to see that the complexity of Algorithm 1 is  $\mathcal{O}(n^2)$ , where  $n$  is the number of macro segments of a path.

#### 4.4 Discussion on the Zero Energy Phenomenon

By the above optimality structure, at the end of each chunk, the remained energy is zero. People may claim that it is not safe to leave the EV with zero energy during a trip. Actually, this is not a problem. In practice, one can

charge the EV batteries with some initial energy for safety. As shown in the proofs of Theorem 1 – 3, the optimization procedure is not affected by the value of initial energy ( $E_0$ ). In problem solving, we treat the non-zero initial energy as zero and then perform speed planning. The result is that the initial energy is still remained in the battery at the end of the trip, i.e., the EV only uses solar energy collected on the way.

## 5. EXPERIMENTS

In this section, we present two sets of experiments:

- simulations are conducted to compare the performance of our proposed method and that of a constrained non-linear programming solver in MATLAB;
- experiments are conducted on a solar-powered EV prototype. The purpose is to evaluate whether our approach can be applied in real-life scenarios.

**Table 1: Simulation results**

| No. | Macro Segments | Length (km) | Travel Time (min) | OPT (sec) | GS (sec) |
|-----|----------------|-------------|-------------------|-----------|----------|
| 1   | 2              | 3.9         | 44.56             | 2         | 3        |
| 2   | 2              | 5.3         | 67.14             | 3         | 34       |
| 3   | 3              | 16.3        | 193.24            | 3         | 34       |
| 4   | 4              | 13.2        | 147.94            | 8         | 158      |
| 5   | 5              | 13.3        | 145.62            | 30        | 125      |
| 6   | 6              | 9.8         | 105.25            | 18        | 152      |
| 7   | 7              | 9.5         | 105.10            | 23        | 174      |
| 8   | 8              | 11.5        | 129.83            | 90        | 129      |
| 9   | 9              | 11.7        | 127.56            | 58        | 1076     |
| 10  | 10             | 12.7        | 138.49            | 98        | 937      |
| 11  | 11             | 15.7        | 169.45            | 64        | 1151     |
| 12  | 12             | 19.1        | 218.15            | 78        | 827      |
| 13  | 13             | 20.3        | 227.22            | 122       | 1044     |
| 14  | 14             | 22.9        | 271.81            | 123       | 2430     |
| 15  | 15             | 27.8        | 314.45            | 106       | 2900     |
| 16  | 16             | 20.4        | 235.60            | 150       | 8215     |
| 17  | 17             | 28.0        | 321.48            | 153       | 9441     |
| 18  | 18             | 24.8        | 286.20            | 171       | 4788     |
| 19  | 19             | 28.7        | 330.35            | 200       | 9436     |
| 20  | 20             | 27.5        | 314.46            | 278       | N/A      |

### 5.1 Simulation Results

In the simulations, we compare the performance of the following two approaches that can find the optimal speed assignment for a path:

- *GlobalSearch* is a constrained non-linear programming solver provided by the MATLAB Global Optimization Toolbox citegs-malab. It applies the scatter search algorithm [35] to generate a number of trial points, then repeatedly examines the trial points and calls another local optimal solver *fmincon* to search the state space.
- *Our approach* applies Algorithm 1 to compute the optimal solution. In the step to compute  $t_{cs}(i, j)$  for a chunk, we apply the *GlobalSearch* solver.

Both approaches are implemented and run within MATLAB 2015a. The maximal allowed iterations is set to 10,000, and the maximal allowed function evaluations are set to 1,000,000 for GlobalSearch, to make both approaches achieve the best quality solution. The experiments run on a desktop computer with a 3.60GHz Intel Core i7-4790 CPU and 16GB main memory. In our simulations, solar input is set to 200W, a common level at around 10:00am on a clear spring day in Shenyang, China. We randomly generate 20 paths with the number of macro segments ranging from 2 to 20, shown in Table 1. The total lengths and the computed minimal travel times (same for both methods) are listed as well. The computation times to solve the optimization problem by our approach, denoted by OPT, and by GlobalSearch, denoted by GS, are shown in the last two columns. If an approach does not finish within 3 hours, we say it runs out of time, and its performance is marked “N/A”.

For analysis time, our approach basically follows the  $\frac{n^2}{2}$  curve, because it computes the travel time of  $\frac{n(n-1)}{2}$  possible chunks (line 2-10 in Algorithm 1). The computation overhead of GlobalSearch increases much faster with the number of segments, basically follows an exponential curve. Our approach wins because we decompose (by the optimal structure) the original problem into smaller sub-problems that can be solved much more efficiently.

## 5.2 Validation Results

To check whether the proposed method applies in complicated real-life situations, we built a small solar-powered EV as a validation platform. The prototype is based on an experimental EV; the major modification is the solar energy system. Figure 3 shows the prototype, the main details of which are listed in Table 2.

**Table 2: Configurations of the solar-Powered EV**

| Component        | Specifications   |
|------------------|--|
| Solar Panel      | Brand: Yingli Solar<br>Module Type: YL270C-30b (60 Cells)<br>Technology: Monocrystalline<br>Power Output (STC): 270W<br>Module Efficiency: 16.6%<br>Cell Dimensions: 156 X 156 (mm)<br>Dimensions: 1640 X 990 X 40 (mm)<br>Weight: 18.5kg        |
| MPPT Controller  | Brand: victron energy<br>Module: BlueSolar MPPT 100/50<br>Output Voltage: 12/24V<br>Rated Charge Current: 50A<br>Max. Power: 700W@12V, 1400W@24V<br>Max. Efficiency: 98%<br>Charging Method: multi-stage adaptive<br>MPPT Control Algorithm: N/A |
| Electric Vehicle | Dimensions: 2050 X 1220 X 1570 (mm)<br>Kerb Mass: 580kg<br>Drive Type: Rear wheel<br>Motor Type: Brushless DC motor<br>Rated Motor Power: 2.2kW<br>Maximum Speed: 35km/h   |

Speed planning requires to know the parameters for the EV power output function, i.e.,  $a$  and  $b$  in equation (7). In

**Figure 3: The solar-powered EV prototype**



(a) Front view

(b) Rear view

reality, the values are determined by many complex factors, such as vehicle specifications, road conditions, weather, etc. To obtain a precise model for the EV output, we use the prototyped platform to profile the required parameters. We collect data on the output power for different speeds, then use the **ctool** in MATLAB to fit a function in the form of equation (7). Then the precise values  $a = 0.01$  and  $b = 33$  specific to our EV and the test roads are obtained.

We conducted four validation experiments in late April, among which three were run on a clear day and one on a cloudy day. The paths were planned on university campus located at latitude  $41^{\circ}76'$  N and longitude  $123^{\circ}42'$  E. On campus, shadings are mainly created by buildings, and we measured the length of each shading segment. On general city areas, with geographical and building data, one can apply the ray-tracing technique to compute the shadings on the road given the current time and location (to compute sun angle). Existing GIS tools (e.g., ArcGIS [3]) are already capable of this computation.

In each experiment, we measure the transient PV input power at the start time, used as the constant input power for the speed planner. Then for a given path, the speed planner returns the optimal speed on each road segment. In each experiment, we drive the EV at the planned speed, and track down the travel time, harvested and consumed energy regarding each road segment. The path configuration and the collected data are listed from Table 3 to Table 6, in which **OPT** and **HW** refer to the results from the speed planner and the real solar EV, respectively.

**Table 3: Validation results for Exp-1**

| Weather: Clear |             | PV Power: 210W    |       | Test Time: 10:32:02 ~ 11:15:44 |        |                    |        |
|----------------|-------------|-------------------|-------|--------------------------------|--------|--------------------|--------|
| Seg.           | Length (km) | Travel Time (min) |       | Energy Input (Wh)              |        | Energy Output (Wh) |        |
|                |             | OPT               | HW    | OPT                            | HW     | OPT                | HW     |
| $S_1^I$        | 1.76        | 23.59             | 23.80 | 82.55                          | 78.17  | 58.43              | 66.38  |
| $S_1^S$        | 0.54        | 1.48              | 1.55  | 0                              | 1.29   | 20.42              | 21.18  |
| $S_2^I$        | 1.22        | 16.35             | 16.82 | 57.22                          | 58.01  | 40.50              | 49.60  |
| $S_2^S$        | 0.54        | 1.48              | 1.55  | 0                              | 1.33   | 20.42              | 22.89  |
| Total          | 4.06        | 42.90             | 43.72 | 139.77                         | 138.80 | 139.77             | 160.05 |

In the first three clear day experiments, experimental data between **OPT** and **HW** match well. The data can be explained in detail from several aspects.

**Table 4: Validation results for Exp-2**

| Weather: Clear                 |             | PV Power: 210W    |       |                   |       |                    |       |
|--------------------------------|-------------|-------------------|-------|-------------------|-------|--------------------|-------|
| Test Time: 11:20:52 ~ 11:40:38 |             |                   |       |                   |       |                    |       |
| Seg.                           | Length (km) | Travel Time (min) |       | Energy Input (Wh) |       | Energy Output (Wh) |       |
|                                |             | OPT               | HW    | OPT               | HW    | OPT                | HW    |
| $S_1^I$                        | 0.53        | 9.05              | 9.55  | 31.66             | 33.56 | 17.68              | 23.73 |
| $S_1^S$                        | 0.34        | 0.93              | 0.87  | 0                 | 0.86  | 12.82              | 15.05 |
| $S_2^I$                        | 0.50        | 8.44              | 8.23  | 29.52             | 26.61 | 16.50              | 20.44 |
| $S_2^S$                        | 0.38        | 1.03              | 1.13  | 0                 | 1.19  | 14.18              | 19.32 |
| Total                          | 1.75        | 19.45             | 19.78 | 61.18             | 62.22 | 61.18              | 78.54 |

**Table 5: Validation results for Exp-3**

| Weather: Clear                 |             | PV Power: 180W    |       |                   |        |                    |        |
|--------------------------------|-------------|-------------------|-------|-------------------|--------|--------------------|--------|
| Test Time: 12:57:26 ~ 13:56:37 |             |                   |       |                   |        |                    |        |
| Seg.                           | Length (km) | Travel Time (min) |       | Energy Input (Wh) |        | Energy Output (Wh) |        |
|                                |             | OPT               | HW    | OPT               | HW     | OPT                | HW     |
| $S_1^I$                        | 0.67        | 18.51             | 18.28 | 55.52             | 58.11  | 22.21              | 30.23  |
| $S_1^S$                        | 0.81        | 2.34              | 2.37  | 0                 | 2.38   | 30.24              | 30.94  |
| $S_2^I$                        | 0.39        | 10.57             | 10.78 | 31.72             | 35.19  | 12.69              | 20.41  |
| $S_2^S$                        | 0.34        | 0.98              | 0.85  | 0                 | 0.84   | 12.69              | 13.72  |
| $S_3^I$                        | 0.36        | 9.91              | 9.63  | 29.74             | 29.85  | 11.90              | 15.42  |
| $S_3^S$                        | 0.38        | 1.09              | 1.17  | 0                 | 1.12   | 14.19              | 17.77  |
| $S_4^I$                        | 0.27        | 7.49              | 7.23  | 22.47             | 22.54  | 8.99               | 11.91  |
| $S_4^S$                        | 0.50        | 1.44              | 1.40  | 0                 | 1.39   | 18.67              | 21.11  |
| $S_5^I$                        | 0.24        | 6.61              | 5.82  | 19.83             | 17.24  | 7.93               | 10.08  |
| $S_5^S$                        | 0.53        | 1.53              | 1.67  | 0                 | 1.59   | 19.77              | 22.72  |
| Total                          | 4.49        | 60.47             | 59.20 | 159.28            | 170.25 | 159.28             | 194.31 |

*Travel time.* There is a slight difference between the travel times predicted by the speed planner and those by the hardware platform. This is because currently our prototyped EV relies on the driver to maintain constant speed. The accuracy of the speedometer, the sensitivity of the acceleration pedal, and the driver’s level of technique introduce inevitable errors during the control process. For advanced EVs with auto-cruise systems, stabilizing speed will be much easier.

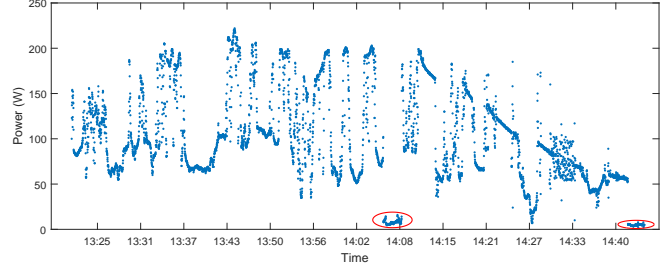
*Collected energy.* Basically, the predicted energy input by the speed planner is very close to that actually collected. This shows that the constant solar power input model is reasonable, at least for the time of the experiments (10:30am - 2:00pm) in which solar power does not change significantly. For Exp-1, the actual collected energy should be larger than the predicted amount, with the change of solar angle. This trend can be witnessed in most illuminated segments. But, on segment  $S_1^I$ , the actually collected energy is lower. This is because the shade of roadside trees on some illuminated segments slightly decreases power input. For Exp-3, the predicted energy input should be larger than the actual data, since solar power decreases in the afternoon. In the experiment, we input a conservative low solar power (180W) to the speed planner to ensure safe predictions, which leads to underestimated solar energy input.

*Consumed energy.* For all three clear day experiments, the average consumed energy is about 20% higher than the prediction. This is the result of two facts: first, acceleration energy consumption is neglected in our model; second, since in illuminated segments the planned speed is 2-3km/h, it is very hard to manually stabilize the speed in this range, which introduces unpredictable acceleration energy.

Comparably, our speed planner works slightly worse in Exp-4, in which the predicted solar energy input is much

**Table 6: Validation results for Exp-4**

| Weather: Cloudy                |             | $E_0$ : 60Wh      |       | PV Power: 60W     |        |                    |        |
|--------------------------------|-------------|-------------------|-------|-------------------|--------|--------------------|--------|
| Test Time: 13:21:26 ~ 14:44:12 |             |                   |       |                   |        |                    |        |
| Seg.                           | Length (km) | Travel Time (min) |       | Energy Input (Wh) |        | Energy Output (Wh) |        |
|                                |             | OPT               | HW    | OPT               | HW     | OPT                | HW     |
| $S_1^I$                        | 1.76        | 45.12             | 45.05 | 45.12             | 87.12  | 58.18              | 76.75  |
| $S_1^S$                        | 0.54        | 2.24              | 2.65  | 0                 | 0.35   | 18.95              | 19.73  |
| $S_2^I$                        | 1.22        | 31.28             | 32.70 | 31.28             | 48.76  | 40.33              | 51.40  |
| $S_2^S$                        | 0.54        | 2.24              | 2.38  | 0                 | 0.19   | 18.94              | 18.64  |
| Total                          | 4.06        | 80.88             | 82.78 | 76.40             | 136.42 | 136.40             | 166.52 |


**Figure 4: Irradiance profile for EXP-4**

lower than the actual input. This is because the weather was unpredictable on that cloudy day. Figure 4 shows the transient solar power profile where the circled areas correspond to the shaded segments. When the experiment started, the solar power decreased to 60W due to dense cloud. We input this small number to the speed planner. However, the cloud cleared up during the trip, and more energy was then harvested. Exp-4 shows that unpredictable weather conditions is a major obstacle for off-line prediction of solar input. Online control will be helpful to deal with such uncertainties by dynamically adjusting the speed plan.

## 6. DISCUSSIONS ON PRACTICAL IMPLEMENTATIONS

In this section, we discuss practical aspects of the proposed framework.

### 6.1 Uncertainties from the Environment

First, solar input is sometimes unpredictable due to weather conditions. Figure 4 shows such an extreme example of cloudy weather. To model complex weather conditions, new frameworks are required. For example, weather inaccuracies can be modeled by stochastic formulation [22] with existing solar power data [2]; then solar power estimations can be obtained by a stochastic optimization procedure. Second, unpredictable traffic situations could make the problem very complex. For instance, when there are traffic jams, the EV has to run much slower on the jam road segment and cannot follow the planned speed. The effects are different when the EV is jammed in illuminated segments or shaded segments. For the former case, more energy could be collected during the trip; for the latter case, if the sun angle is decreasing, the travel time for the remaining trip will be increased since solar power is lower. Since the locations of traffic jams are in general changing over time, such uncertainties are very hard to model, and thus it is not possible to obtain optimal speed assignment statically.

## 6.2 Solar Input and Acceleration Energy

In this paper, we use a constant solar power in energy input prediction. In real-time, solar power is continuously changing with the change of sun angle during the trip. Energy input now has a more complex relation with the car speed. Regarding energy output, we used a simpler model where acceleration energy is ignored. Validation results (in Sec. 5.2) show that even if we simplified energy input/output models, the analysis precision is good enough for some practical use, such as short-range trips.

## 6.3 Potential Application Scenarios

Given the state-of-the-art efficiency of solar panels and typical energy loss, energy harvesting on a clear summer day is about 2KWh for a  $1.6m^2$  panel (used in our validation). Take NISSAN Leaf [4] for example, 2KWh can support a 11.6km range. As the energy is harvested in about 10 hours, the average speed is 1.16km/h. We acknowledge that purely relying on solar energy is not a reasonable solution for an ordinary EV in daily use.

For light-weight low-speed EVs, like the prototype in this paper, 2KWh may support up to 25km range (an average speed of 2.5km/h). Note that the highest efficiency achieved in labs is up to 46% [5]; once commercialized, daily energy harvesting of a solar panel can be up to 5.54KWh, supporting a range of 70km. If we extend the area of the solar panel to  $2.3m^2$ , the average speed will be up to 10km/h, which is actually the average speed in rush hours in a densely populated Chinese city. As reported in [6], the market of low-speed EVs in China was increased by 46.6% in 2013, mainly because they are cheap, small, and enough for low-end use. The proposed solution will become more applicable in the future for this special yet fast increasing EV market.

## 7. RELATED WORK

In a closely related work [26], Plonski et al. studied the problem of path planning for solar-powered robots. The main objective is to select a path from a map and assign speeds to the path segments so that the energy consumed for the trip is minimized with given timing constraints. The focus of the work was on precisely modeling solar radiance over the interested area, which can be used to improve the precision of solar power modeling of our work in the future. In another work [30], Sorrentino et al. studied energy optimization of an electric vehicle powered by both solar panels and batteries. They used genetic algorithm to find a speed profile that minimizes the overall energy consumption of a trip. However, Sorrentino’s work does not consider the shadings on a path, so their problem is essentially different from the problem studied in this paper.

A large body of research work focuses on path planning of solar-powered aircrafts [19, 31, 20, 13, 17, 12, 25], mostly Unmanned Aerial Vehicles (UAVs). The general objective is to maximize solar energy harvesting for a trip within hours. Different from road vehicles, the controller may adjust not only the speed but also the heading angle and the bank angle to optimize the solar irradiance input angle for higher power collection. Path optimization is conducted to cope with complex solar irradiance distribution due to local weather. Essentially, these problems have different energy harvesting and power consumption models from our problem. Path planning for aircrafts basically allows an aircraft to bypass low solar power areas; for our problem, it is generally not

possible to bypass the shaded segment on a selected path, and the planner must carefully assign vehicle speed to successfully survive the “dark” segments.

Some researchers studied the path and speed planning problem for non-solar-powered electric vehicles [8, 9, 33, 32, 28, 14]. A common optimization objective is to minimize energy consumption by finding the right path between two locations and assign optimal speeds on different parts of the route. Most of the problems can be formulated as the Constrained Shortest Path (CSP) problem [18] which is known to be NP-complete [16]. The solutions are subject to certain constraints, such as overall trip time, battery capacity, the number of recharging stations on the route [32, 28], etc. A fundamental difference between our work and these research is that the related works do not consider solar energy input during the trip. Exceptionally, some research considers energy recuperation in their models [8, 9], which is similar to the solar energy input on illuminated road segments in our model. However, the two types of models are essentially different: those in [8, 9] assume fixed energy input on a road segment; while in our model, the amount of solar energy input depends on the speed assignment to the corresponding road segment, which is generally further affected by the solar input along the whole path.

Related work also considered speed planning to improve comfort during driving [21, 34]. Specifically, such problems aim at reducing the level of accelerations and longitude jerk by optimizing the speed and trajectory of the vehicle for a path with specific road conditions. These research problems require more detailed information on vehicle propelling and road conditions, but neither timing requirements nor energy harvesting/consumption is within their concern.

The design of solar cars has been extensively explored in worldwide challenges, e.g., the famous American Solar Challenge [1]. In these challenges, the designers mainly focus on maximizing the area of solar panels and optimizing the car shape for best aerodynamic performance, so that the solar car can achieve an as long as possible range with a decent speed. These challenges greatly motivates the use of solar energy on EVs; however, the proposed EV models are still not suitable for nowadays real-life use.

## 8. CONCLUSION & FUTURE WORK

We have studied the speed planning problem for solar-powered EVs to successfully finish a trip with minimal travel time. The problem is a constrained non-linear programming problem with many variables, which is generally very hard to solve. By exploring the optimality structure of this specific problem, we propose a dynamic-programming-based method to efficiently compute the optimal speed assignment for a trip. Simulation results show that our approach can significantly improve analysis performance compared to the state-of-the-art approaches. Validation results on a solar-powered EV prototype demonstrate that the proposed method can be used in some real-life scenarios.

In the future, we plan to improve the proposed framework from the following aspects: (1) incorporating variable solar power, variable shadings and acceleration energy consumption for better modeling/analysis precision; (2) new frameworks to model uncertain weather and traffic situations; (3) integrating map applications, shading analysis and speed planning into an in-car mobile application.

## 9. REFERENCES

- [1] <http://americansolarchallenge.org/>.
- [2] <http://umbra.nascom.nasa.gov/sdac.html>.
- [3] <http://www.esri.com/software/arcgis/>.
- [4] <http://www.nissanusa.com/electric-cars/leaf/>.
- [5] <http://www.nrel.gov/ncpv/>.
- [6] <http://www.researchinchina.com>.
- [7] Ministerial, clean energy. global ev outlook understanding the electric vehicle landscape to 2020. *Clean Energy Ministerial Report 1*, 2013.
- [8] A. Artmeier, J. Haselmayr, M. Leucker, and M. Sachenbacher. The optimal routing problem in the context of battery-powered electric vehicles. In *2nd International Workshop on Constraint Reasoning and Optimization for Computational Sustainability*, 2010.
- [9] M. Baum, J. Dibbelt, T. Pajor, and D. Wagner. Energy-optimal routes for electric vehicles. In *Proceedings of the 21st ACM SIGSPATIAL International Conference on Advances in Geographic Information Systems*, pages 54–63, 2013.
- [10] M. S. Bazaraa, H. D. Sherali, and C. M. Shetty. *Nonlinear programming: theory and algorithms*. John Wiley & Sons, 2013.
- [11] D. Block and J. Harrison. Electric vehicle sales and future projections. *Electric Vehicle Transportation Center, EVTC Report Number: EVTC-RR-01-14*, January 2014.
- [12] R. Dai. Path planning of solar-powered unmanned aerial vehicles at low altitude. In *Circuits and Systems (MWSCAS), 2013 IEEE 56th International Midwest Symposium on*, pages 693–696, Aug 2013.
- [13] R. Dai, U. Lee, S. Hosseini, and M. Mesbahi. Optimal path planning for solar-powered uavs based on unit quaternions. In *IEEE 51st Annual Conference on Decision and Control*, 2012.
- [14] W. Dib, A. Chasse, P. Moulin, A. Sciarretta, and G. Corde. Optimal energy management for an electric vehicle in eco-driving applications. *Control Engineering Practice*, 29:299–307, 2014.
- [15] M. Ehsani, Y. Gao, and A. Emadi. *Modern Electric, Hybrid Electric, and Fuel Cell Vehicles: Fundamentals, Theory, and Design (2nd Edition)*. CRC Press, 2010.
- [16] M. R. Garey and D. S. Johnson. *Computer and intractability: A Guide to the Theory of NP-Completeness*. W. H. Freeman, 1979.
- [17] S. Hosseini, R. Dai, and M. Mesbahi. Optimal path planning and power allocation for a long endurance solar-powered uav. In *American Control Conference (ACC), 2013*, pages 2588–2593, June 2013.
- [18] H. C. Joksch. The shortest route problem with constraints. *Journal of Mathematical analysis and applications*, 14(2):191–197, 1966.
- [19] A. T. Klesh and P. T. Kabamba. Energy-optimal path planning for solar-powered aircraft in level flight. In *AIAA Guidance, Navigation and Control Conference and Exhibit*, August 2007.
- [20] A. T. Klesh and P. T. Kabamba. Solar-powered aircraft: Energy-optimal path planning and perpetual endurance. *Journal of Guidance, Control, and Dynamics*, 32(4), 2009.
- [21] L. Labakhua, U. Nunes, R. Rodrigues, and F. S. Leite. Smooth trajectory planning for fully automated passengers vehicles: Spline and clothoid based methods and its simulation. *Informatics in Control Automation and Robotics*, pages 169–182, 2008.
- [22] S. Mohanty, P. K. Patra, and S. S. Sahoo. Prediction and application of solar radiation with soft computing over traditional and conventional approach – a comprehensive review. *Renewable and Sustainable Energy Reviews*, 56:778 – 796, 2016.
- [23] D. R. Myers. *Solar radiation: practical modeling for renewable energy applications*. CRC Press, 2013.
- [24] J. Neubauer and E. Wood. The impact of range anxiety and home, workplace, and public charging infrastructure on simulated battery electric vehicle lifetime utility. *Journal of Power Sources*, 2014.
- [25] E. E. Pinar. Energy optimal path planning of an unmanned solar powered aircraft. *a thesis of Middle East Technical University*, 2013.
- [26] P. A. Plonski, P. Tokekar, and V. Isler. Energy efficient path planning for solar-powered mobile robots. *Journal of Field Robotics*, 30(4):583–601, 2013.
- [27] G. Rizzo and I. Arsie. Solar energy for cars: perspectives, opportunities and problems. In *GTAA Meeting*, May 2010.
- [28] M. Schneider, A. Stenger, and D. Goeke. The electric vehicle-routing problem with time windows and recharging stations. *Transportation Science*, 48(4):500 – 520, 2014.
- [29] R. Singh, M. K. Gaur, and C. S. Malvi. Study of solar energy operated hybrid mild cars: A review. *International Journal of Scientific Engineering and Technology*, 1:139 – 148, 2012.
- [30] Sorrentino, M., Arsie, I., Di Martino, R., and Rizzo, G. On the use of genetic algorithm to optimize the on-board energy management of a hybrid solar vehicle. *Oil Gas Sci. Technol. – Rev. IFP*, 65(1):133–143, 2010.
- [31] S. C. Spangelo, E. G. Gilbert, A. T. Klesh, P. T. Kabambax, and A. R. Girard. Periodic energy-optimal path planning for solar-powered aircraft. In *AIAA Guidance, Navigation, and Control Conference*, 2009.
- [32] S. Storandt. Quick and energy-efficient routes: computing constrained shortest paths for electric vehicles. In *Proceedings of the 5th ACM SIGSPATIAL International Workshop on Computational Transportation Science*, pages 20–25, 2012.
- [33] M. Targosz, M. Szumowski, W. Skarka, and P. Przystalka. Velocity planning of an electric vehicle using an evolutionary algorithm. *Activities of transport telematics*, pages 171 – 177, 2013.
- [34] J. Villagra, V. Milanés, J. Perez, and J. Godoy. Smooth path and speed planning for an automated public transport vehicle. *Robotics and Autonomous Systems*, 60(2):252–265, 2012.
- [35] U. Zsolt, L. Lasdon, J. Plummer, F. Glover, J. Kelly, and R. Marti. Scatter search and local nlp solvers: A multistart framework for global optimization. *INFORMS Journal on Computing*, 19(3):328 – 340, 2007.